THE ROLE OF QUANTUM MECHANICS IN NEUTRINO FACTORIES

JUAN C. GALLARDO
Brookhaven National Laboratory, Upton NY 11973, USA
E-mail: gallardo@bnl.gov

ANDREW M. SESSLER
Lawrence Berkeley National Laboratory, Berkeley, CA 94720, USA
E-mail: amsessler@lbl.gov

JONATHAN WURTELE
University of California and Lawrence Berkeley National Laboratory, Berkeley, CA 94720, USA
E-mail: wurtele@physics.berkeley.edu

A compilation is made of the various ways in which quantum phenomena enter into the design and operation of a neutrino factory. They include production of pions, decay of pions into muons, ionization energy loss of muons in material, scattering and energy straggling of muons in material, polarization of muons, and the decay of muons into neutrinos, and the radiation effect of neutrinos. For each process formulas are presented which cover the basic mechanism. A discussion is presented of the areas of uncertainty and of the experiments, underway and proposed, which will reduce the uncertainty to an acceptable level.

1 Introduction

All existing accelerators and storage rings for protons and electrons are based upon classical considerations. That is, quantum mechanics plays a small, essentially negligible, role. The very hard radiation from synchrotron radiation sources must be treated quantum mechanically, but that is more a performance than a design matter. In all devices, the multiple scattering of beams from gas molecules is a quantum effect, but by making the vacuum good enough, and that is exactly what is done in practice, the effect can be made negligible.

In contrast, a Neutrino Factory [12], relies upon quantum mechanics in a variety of ways and, all of these aspects are crucial to the operation of the device. In this way, a Neutrino Factory is distinctly different from other accelerators and storage rings.

We compile these various phenomena and give formulas that cover each case. There is nothing new here, in the sense that neutrino factory designers

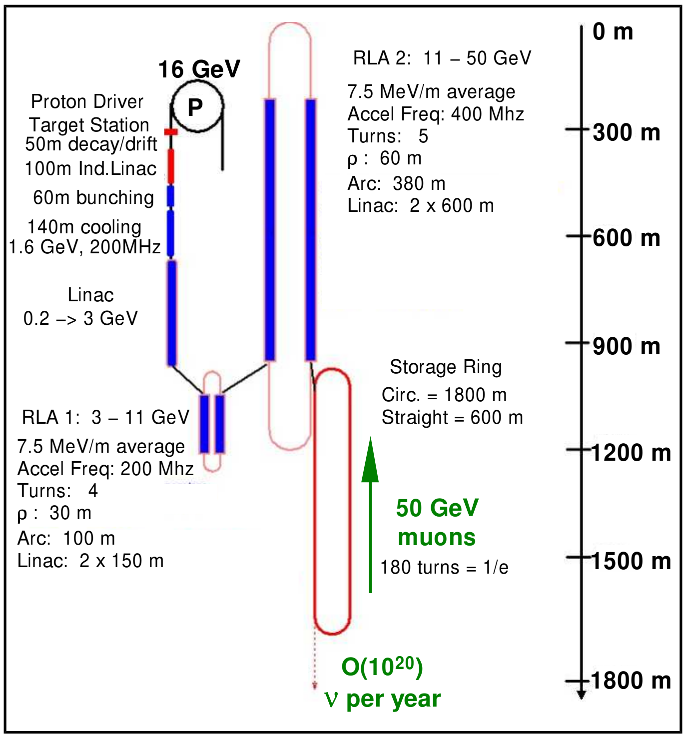

Figure 1. A general layout of a Neutrino Factory.

know all these things, but it is interesting, especially for the outsiders, to look at the proposed factory from this point of view and to put down, in one place, the various quantum mechanical effects.

Finally, a discussion is given of the uncertainty in the formulas presented and experiments, underway and proposed, to reduce the uncertainty to an acceptable level. A general layout of a Neutrino Factory is shown in Fig. 1,

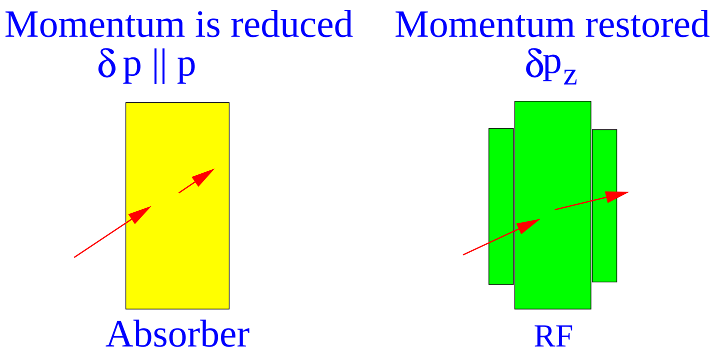

Figure 2. The principle of ionization cooling. Notice how the result of absorption and acceleration is a reduction in transverse momentum, i.e. *cooling*

courtesy of S. Geer, C. Johnstone and D. Neuffer [3]. The design of a Neutrino Factory is dominate by two aspects; firstly, muons ($\mu's$) are produced in a diffuse phase space and they decay rapidly ($\tau \approx 2.19703 \times 10^{-6}\ s$); as a result it is needed,

High power (1 to 4 MW) proton beam	Efficient production and capture
Rapid cooling	Acceleration
Lattice for tilted storage ring	Many engineering issues

The heart of a Neutrino Factory is transverse cooling (longitudinal cooling is not needed). The only known cooling method that is fast enough is *ionization cooling* [4]. Close to a factor of 10 in muon intensity is developed in this way; a schematic of the method is shown in Fig. 2.

2 Pion Production

The prefered method of pion production is to bring a high energy proton beam on a heavy metal target; the copious pion yield is mainly from the excitation of the $\Delta(3,3)$ resonance as seen in Fig. 3.

In the region of low kinetic energy significant capture can be achieved by immersing the production target in a high-field solenoid of large bore. Pions of both signs having transverse momentum of up to 225 MeV/c are focused into the decay channel via matching solenoids. It is worth to note that the pion normalized velocity varies from 0.68 to 0.98.

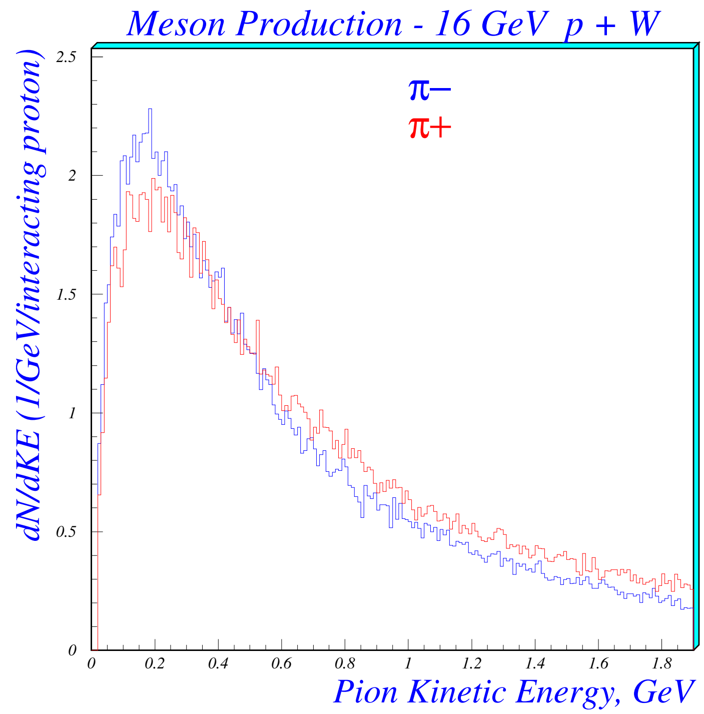

Figure 3. Energy distribution of pions produced by 16 $\frac{\mathrm{GeV}}{\mathrm{c}}$ protons on a tungsten target of optimal length. The curves are phenomenological fits of experimental data extrapolated to low pion energy.

In Fig. 4, courtesy of H. Kirk[5] we display experimental data on pion production and its comparison with the production code MARS[6].

In Fig. 5, courtesy of K. McDonald [7] we show a schematic of the target and capture region of a Neutrino Factory.

3 Pion Decay $\pi \longrightarrow \mu + \nu_\mu$

Pion decay is isotropic in the pion frame, with a lifetime of 2.9×10^{-8} s; the resulting muons are completely polarized, i.e. the spin is aligned with the momentum in the pion rest frame. Therefore, there is an energy dependence of the muon polarization in the laboratory frame. If all the pions moved with the same velocity, there would be distinct polarization associated with

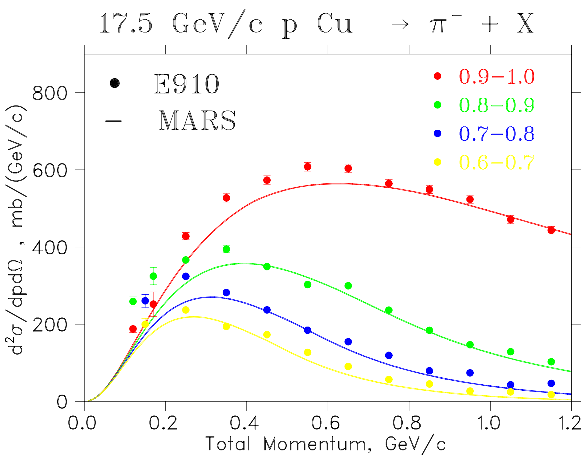

Figure 4. Experimental data from BNL-E910 at Brookhaven National Laboratory. The solid curves, labeled by the cosine of the production angle, are results from the production code MARS.

each muon energy. However, the velocity spread of pions removes the exact correlation of polarization with muon energy; consequently, the insertion of an rf cavity near the pion source (e.g., target) can create a more mono-energetic pion beam and, therefore, more correlation between the polarization and the energy of the muon beam.

4 Energy Loss of Muons in Material

The energy loss of muons, as they travel through material, leads to a reduction in transverse (normalized) emittance given by

$$\frac{d}{ds}\epsilon_T = -\frac{\epsilon_T}{\beta cp}\left|\frac{dE}{ds}\right|. \tag{1}$$

The energy loss in different materials [8] is shown in Fig. 6

At the same time, there is longitudinal emittance growth given by,

$$\frac{d\epsilon_L}{ds} \approx \epsilon_L \frac{d}{dE}\left(\frac{dE}{ds}\right) + ..., \tag{2}$$

i.e. the low energy particles lose more energy. In addition there are stochastic phenomena both transversely (see Sec. 5) and longitudinal (see Sec. 6)

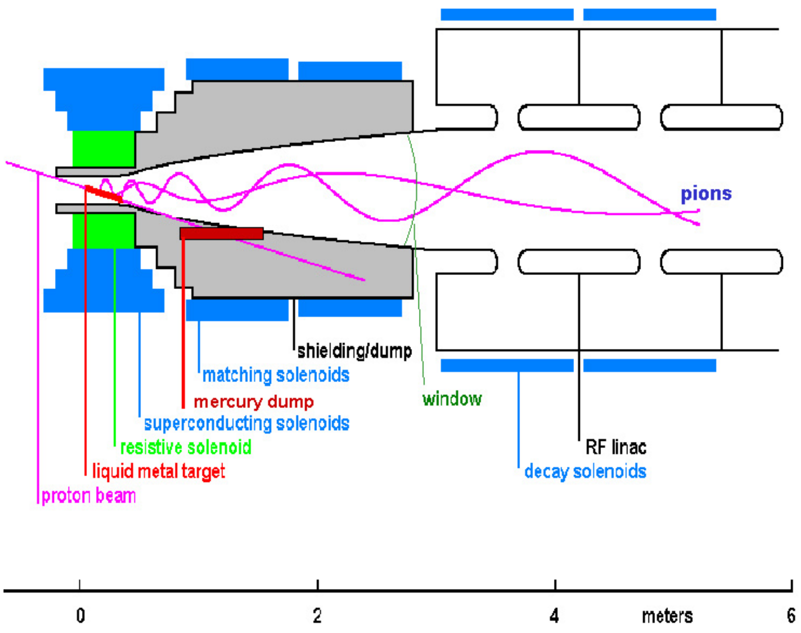

Figure 5. A 4 MW, 16 GeV/c, proton beam hits a liquid metal target in a 20 T solenoid. Pions and (then muons) are captured in a decay channel

5 Scattering of Muons

Multiple scattering leads to a Gaussian distribution whose *rms* angular dependence is

$$\sqrt{<\theta^2>} = \sqrt{\theta_c^2 L} \quad \text{where} \quad \theta_c^2 = \left(\frac{0.014[GeV]}{\beta c p}\right)^2 \frac{1}{L_R}, \tag{3}$$

and L_R is the radiation length of the material.

A muon beam going through material has its transverse (normalized) emittance ϵ_T altered by both energy loss and multiple scattering,

$$\frac{d\epsilon_T}{ds} = -|\frac{dE}{ds}|\frac{\epsilon_T}{\beta^2 E} + \frac{1}{2}\frac{\gamma\beta}{\epsilon_T}{\sigma_r}^2\frac{d<\theta^2>}{ds^2}. \tag{4}$$

The minimum emittance is obtained by equating the two terms on the right

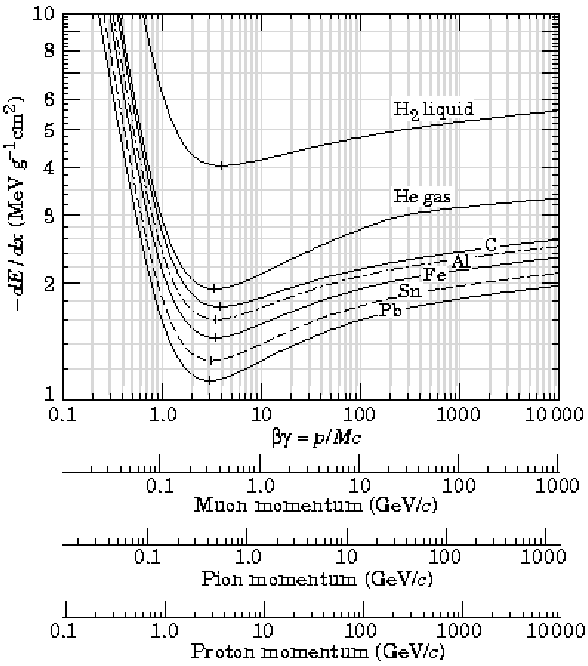

Figure 6. Energy loss of muons in different materials.

side of Eq. 4, and using Eq. 3:

$$\epsilon_T(minimum) = \left(\frac{(0.014)^2}{2m_\mu c^2 \beta}\right) \frac{\beta_o}{L_R |\frac{dE}{ds}|}, \tag{5}$$

where β_o is the betatron function. Comparison of various materials is given in Tb. 1.

At small angles, *multiple scattering* yields a Gaussian distribution; at large angles *single scattering* dominates. The intermediate region is called *plural scattering* and has been calculated by Molière, Bethe and others [9]. This formalism requires atomic scattering form factors; usually the Thomas-Fermi model is used to evaluate these factors. For hydrogen this approach is not correct and exact form factors need to be used. Scattering from atomic electrons has often been taken into account by replacing the factor Z^2 in the Molière theory by Z(Z+1); for muons this is not correct, in addition the theory

Table 1. A comparison of materials possible for ionization cooling. Clearly liquid Hydrogen is best.

Material	T °K	Density $\frac{g}{cm^3}$	$\frac{dE}{ds}$ MeV/cm	L_R m	$L_R \frac{dE}{ds}$ MeV
Liquid H	20	0.01	0.29	8.9	258
Liquid He	4	0.13	0.24	7.6	182
LiH	300	0.82	1.60	0.97	155
Li	300	0.53	0.88	1.6	141
Be	300	1.86	2.95	0.35	103
CH2	300	0.96	1.93	0.48	93

assumes that the scattering angle is small ($\sin\theta \approx \theta$) and that the scattering problem is equivalent to a diffusion problem in the angular variable θ.

Consider the classical Rutherford cross section

$$NL\sigma(\chi)\chi d\chi = 2\Xi_{c1}^2 \chi \frac{q(\chi)}{\chi^4} d\chi, \tag{6}$$

where $\Xi_{c1}^2 = 4\pi NL\frac{e^4 Z^2}{(pc\beta)^2}$ with NL the number of atoms per cm^2 in the target, Z the charge of the nucleus and $q(\chi)$ the form factor of the scattering center. This form factor consists of two contributions,

$$q_{el}(\chi) = (1 - f(t))^2 \quad ; \quad q_{inel}(\chi) = 1 - f(t)^2, \tag{7}$$

where $f(t) = \frac{1}{(1-0.25a_o^2 t)^2}$, a_o is the Bohr radius and t is the squared of the momentum transfer. This cross section is employed in the Molière theory.

Taking scattering of all three types and straggling into account requires numerical simulation; an example of this work is shown in Figs. 7, 8.

6 Straggling of Muons

Straggling, Landau straggling, is the spread of energy (a statistical phenomena) as particles loose energy in traversing material. The increased energy spread corresponds to an increase in longitudinal emittance of the muon beam.

Straggling is given by,

$$\frac{d\sigma_{p_z}}{ds} \approx \frac{2\pi\left(\gamma r_\mu m_\mu c^2\right)^2}{\beta c\sigma_E} \frac{N_A Z\rho}{A}\left(1 - \frac{1}{2}\beta^2\right), \tag{8}$$

where m_μ is the muon mass, N_A is the Avogadro's number, Z is the atomic number, ρ is the density and A is the atomic weight.

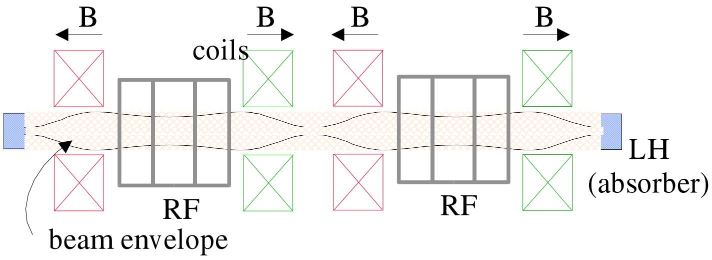

Figure 7. Schematic of a cell in the transverse cooling channel.

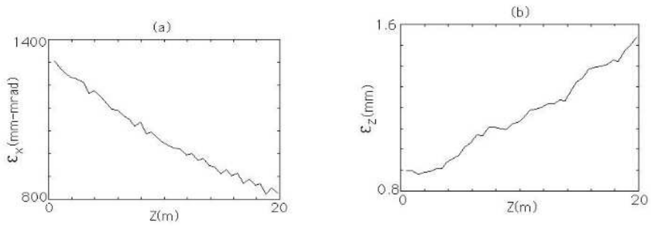

Figure 8. Transverse cooling simulation showing the decrease in transverse emittance and the increase in longitudinal emittance as the muon beam propagates in the cooling channel shown in Fig. 7

In practice, the *wrong* slope of the $\frac{dE}{ds}$ curve at energies where cooling is optimal, gives a larger contribution to the longitudinal emittance (see Sec. 4).

7 Decay of Muons into Neutrinos $\mu^{\pm} \longrightarrow e^{\pm} + \nu_e(\bar{\nu}_e) + \bar{\nu}_\mu(\nu_\mu)$

The cross sections for muon decay, in the muon rest frame, are given by,

$$\begin{aligned} \frac{d^2N_{\nu_\mu}}{dx\,d\Omega_{cm}} &\propto \frac{2x^2}{4\pi}\left[(3-2x)+(1-2x)P_\mu\cos\theta_{cm}\right], \\ \frac{d^2N_{\overline{\nu}_e}}{dx\,d\Omega_{cm}} &\propto \frac{12x^2}{4\pi}\left[(1-x)+(1-x)P_\mu\cos\theta_{cm}\right], \end{aligned} \tag{9}$$

where $x \equiv \frac{2E_\nu}{m_\mu}$, θ_{cm} is the angle between the neutrino momentum vector and the muon spin direction and P_μ is the average muon polarization along the beam direction; the corresponding distributions for $\bar{\nu}_\mu$ and ν_e from μ^+ decay are obtained by replacing $P_\mu \to -P_\mu$.

The neutrino charge current (CC) interaction with matter, for E_ν greater than $\approx$ 10 GeV, are dominated by deep inelastic scattering and are given by

$$\begin{aligned} \sigma(\nu + N \longrightarrow l^- + X) &\approx 0.67 \times 10^{-38} cm^2 E_\nu(GeV), \\ \sigma(\overline{\nu} + N \longrightarrow l^+ + X) &\approx 0.34 \times 10^{-38} cm^2 E_{\overline{\nu}}(GeV), \end{aligned} \tag{10}$$

where $l(e,\mu)$ stands for the corresponding lepton to (ν_e, ν_μ). The neutral current (NC) cross sections are approximately 0.4 of the CC cross sections and are

$$\begin{aligned} \sigma(\nu + N \longrightarrow \nu + X) &\approx 0.3 \times 10^{-38} cm^2 E_\nu(GeV), \\ \sigma(\bar{\nu} + N \longrightarrow \bar{\nu} + +X) &\approx 0.15 \times 10^{-38} cm^2 E_{\overline{\nu}}(GeV). \end{aligned} \tag{11}$$

8 Polarization of Muons

The average muon polarization approaches (in practice) 18.5%. Reducing the energy spread of pions produces (in practice) an increase of the muon beam polarization up to $\approx$ 35 %.

The muon spin vector time evolution is described by the Thomas-BMT equation [10] which is given in Eq. 12

$$\frac{d\vec{S}}{ds} = -\frac{e}{p_z}\vec{\Omega} \times \vec{S}, \tag{12}$$

where

$$\vec{\Omega} = (a\gamma + 1)\vec{B} - a\frac{(\gamma - 1)}{\beta^2}\vec{\beta} \cdot \vec{B}\vec{\beta} + \gamma(a + \frac{1}{\gamma + 1})\vec{E} \times \vec{\beta}, \tag{13}$$

where $\vec{E}, \vec{B}$ are the electromagnetic fields sampled by a muon of normalized velocity $\vec{\beta}$ and normalized energy γ in the laboratory frame. The parameter $a = 1.165 \times 10^{-3}$ is the g-factor anomaly for the muon.

In the cooling channel muons in matter have a finite probability of changing their spin due to: a) Elastic and multiple scattering; b) Energy loss. These effects are determined by computing the first order QED probability for helicity flip. The results of such calculations are shown in Fig. 9.

9 Experiments

There are three production experiments, either completed BNL-AGS-E910 [11] or underway, HARP (CERN) [12] and FNAL P-907 [13], measuring production of pions by protons at energies of 5-120 GeV. There is a scattering experiment

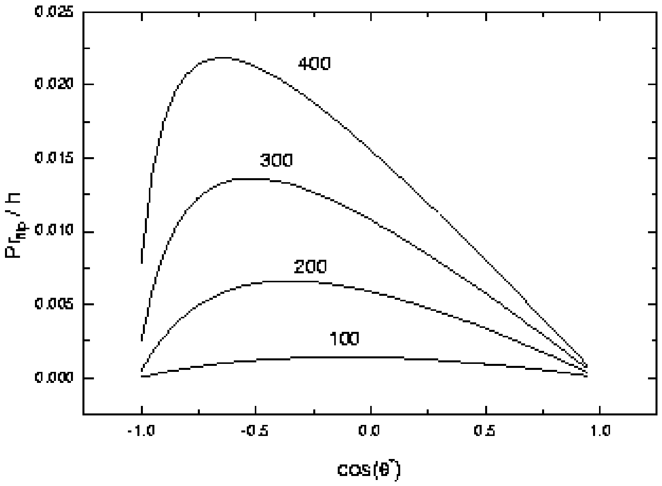

Figure 9. First ordder QED calculation of the probability that a muon scattered through an angle θ^* undergoes a spin flip. The probability is divided by the helicity and the labels indicate the muon momentum in the laboratory frame in Mev/c

being undertaken at TRIUMF (E875) [14], and there is a cooling experiment under design at FNAL [15].

The HARP experiment is the most comprehensive for the region of concern. They plan to have a proton beam of energy range $2 - 24$ GeV/c (1-2 GeV/c steps), and various target of thickness (thin, 1 and 2 interaction lengths) and various materials (Li, Be, C, Al, Ni, Cu, W, liquid Ga-Sn and Hg).

The scattering experiment at TRIUMF will use various targets of different thicknesses,

Liquid Hydrogen, 100 mm and 150 mm
Lithium, 10 mm and 2.5 mm
Beryllium, 2 mm and 0.5 mm
Carbon, 2.5 mm
CH_2, 2 mm
Iron, 0.15 mm and 2 mm

A comprehensive cooling experiment is being considered, efforts are underway to locate and develop a suitable muon beam.

10 Conclusions

The quantum effects in neutrino factories fall into effects due to the strong, the electromagnetic, and the weak interactions.

Strong interaction effects include the production of pions by the initial protons and the radiation effects due to showers initially caused by neutrinos. For both of these effects experimental information is required. Experiments are underway (three) to determine production energy and angular distributions with good accuracy. Radiation effects are adequately understood.

Electromagnetic effects include the energy loss of muons, the scattering of muons and the straggling of muons. In principle, these can be calculated, but material being complicated, experimental information is often used. For hydrogen it should be possible to calculate these phenomena with sufficient accuracy. These phenomena enter into the cooling process and it is intended to demonstrate cooling; i.e., the adequate accuracy of the above phenomena as well as the (much more important) technology and beam handling capability required for cooling.

Weak interaction effects include the decay of pions into muons (and a neutrino) and the decay of muons into two neutrinos (and an electron). These cross sections are precisely known from theory.

Acknowledgments

This research has been supported by the U.S. Department of Energy under Contracts No. DE-AC0298CH10886, No. DE-AC02-76CH03000, and No. DE-AC03-76SF00098. The authors thanks the members of the Neutrino Factory and Muon Collider Collaboration for their contribution to this work.

References

1. A. Sessler, *Neutrino Factories: The Facility*, S. Geer, *Neutrino Factories: Physics*, submitted to *Comments on Nuclear and Particle Physics*; http://www-mucool.fnal.gov/mcnotes/muc0155.pdf and muc0154.pdf; S. Geer, *Phys. Rev.* D **57**, 6989 (1998).
2. Database of technical papers,
http://www-mucool.fnal.gov/notes/notes.html;
Status of Muon Collider R&D and Future Plans,
http://prst-ab.aps.org/abstract/PRSTAB/v2/i8/e081001; *Neutrino Factory Feasibility Study I* ,

`http://www.fnal.gov/projects/muon_collider/nu-factory/`

fermi_study_after_april1st/;

Neutrino Factory Physics Study Group,

http://www.fnal.gov/projects/muon_collider/nu/study/study.html.

3. V.V. Parkhomchuk and A.N. Skrinsky, *Proceedings of the 12th International Conference on High Energy Accelerators*, eds. F.T. Cole and R. Donaldson (Fermilab, Batavia, IL, USA, 1983). http://www-ppd.fnal.gov/muscan/munotes/mc-003.pdf.
4. S. Geer, C. Johnstone and D. Neuffer, *FERMILAB-Pub-99/121* 1999.
5. H. Kirk, *private communication.*
6. N. Mokhov, *The MARS Code System User's Guide*, version 13(95), Reference Manual, Fermilab-FN-628, 1995; http://www-ap.fnal.gov/MARS/.
7. K. McDonald *et al*, *A proposal for an R&D Program for Targetry and Capture at a Muon Collider Source*, http://www.hep.princeton.edu/mumu/target/targetprop.ps.
8. Particle Data Book *et al*, Eur. Phy. J. C **15**, 1 (2000).
9. H. Bethe *et al*, Phys. Rev. **89**, 1256 (1953); Molière, Z. Naturforschg. **3a**, 78 (1948).
10. J. Jackson, *Classical Electrodynamics*; R. Fernow *et al*, *On Muon de-polarization effects in an Ionization Cooling Channel*, http://www-mucool.fnal.gov/mcnotes/muc0115.ps.
11. **BNL-AGS-E910**, *A facility to study proton-nucleus and heavy ion collisions using a large-acceptance detector with particle identification capability*, http://nevis1.nevis.columbia.edu/heavyion/e910
12. **HARP (PS214)**, *The Hadron production Experiment at the PS*, http://harp.web.cern.ch/harp/
13. R. Raja, **FNAL-P907**, private communication.
14. D. Attwood *et al*, **MUSCAT- The Muon Scattering Experiment**, BNL report BNL-67710/CAP-291-Muon-00C.
15. S. Geer *et al*, *MUCOOL Proposal* ,

http://www.fnal.gov/projects/muon_collider/cool/cool.html